Human Pathology (2020) **105**, 20–30

ELSEVIER

Human PATHOLOGY

www.elsevier.com/locate/humpath

Original contribution

Comprehensive molecular genetic studies of Epstein-Barr virus-negative aggressive Natural killer-cell leukemia/lymphoma☆

Juehua Gao, MD, PhD [a,*], Yanming Zhang, MD [b], Nabeel R. Yaseen, MD [a], Yuqiang Fang, MBBS [b], Xinyan Lu, MD [a], Madina Sukhanova, PhD [a], Qing Chen, MD, PhD [a], Yi-Hua Chen, MD [a]

[a] *Department of Pathology, Northwestern University Feinberg School of Medicine, Chicago, IL 60611, USA*
[b] *Department of Pathology, Memorial Sloan Kettering Cancer Center, New York, NY 10065, USA*

Received 20 July 2020; revised 22 August 2020; accepted 25 August 2020

Available online 2 September 2020

Keywords:
Aggressive NK-cell leukemia/lymphoma;
EBV;
Cytogenetics;
Next-generation sequencing (NGS);
SNP microarray

Summary EBV-negative aggressive NK-cell leukemia/lymphoma (ANKL) is a recently recognized, rare NK-cell neoplasm that preferentially affects non-Asians and has a fulminant clinical course. Little is known about the genetic alterations of this disease. In this study, we performed comprehensive molecular genetic studies, including chromosomal analysis, fluorescence in situ hybridization, single nucleotide polymorphism (SNP) microarray, and next-generation sequencing (NGS), on 4 patients diagnosed in our institution. The results demonstrated that our EBV-negative ANKLs have highly complex genomic profiles characterized by near-triploid/near-tetraploid karyotype (3 of 3) with numerous structural abnormalities, inactivation of *TP53* (3 of 3), overexpression of c-Myc (4 of 4), strong expression of PD-L1 in neoplastic cells (2 of 4), and gain of the 11q23-ter region (2 of 2). Our study provides important insights of EBV-negative ANKL, which share many of the genetic features with their EBV-positive counterpart. The strong expression of Programmed death-ligand 1 (PD-L1) suggests that immune checkpoint inhibitors may be further explored as a potential therapeutic option for this highly aggressive, chemotherapy-resistant NK-cell neoplasm.

☆ Disclosure. The authors declare no conflict of interest. Funding: The study is partly supported by Memorial Sloan Kettering Cancer Center Core Grant (P30 CA008748) (YF, YZ).

* Corresponding author. Department of Pathology, Northwestern University Feinberg School of Medicine, Feinberg Pavilion 7-209A, 251 E Huron Street, Chicago, IL 60611, USA.
E-mail address: j-gao@northwestern.edu (J. Gao).

https://doi.org/10.1016/j.humpath.2020.08.008
0046-8177/

1. Introduction

The classic type of aggressive NK-cell leukemia/lymphoma (ANKL) preferentially affects Asians and is highly associated with EBV infection [1]. Most patients have a very aggressive clinical course and are refractory to chemotherapy [1]. The etiology of ANKL remains to be elucidated, but the strong association with EBV infection suggests a pathogenic role for the virus. Previous studies on EBV-positive ANKL demonstrated somatic mutations enriched in the JAK/STAT signaling pathway including *STAT3*, *STAT5*, *JAK2*, *JAK3*, *STAT6*, *SOCS1*, *SOCS3*, and *PTPN11* [2]. In addition, mutations leading to constitutive activation of the RAS-MAPK-ERK pathway have also been reported [3]. A recent study reported 12 cases of ANKL including 9 EBV-positive cases. Five of the 9 cases showed clonal cytogenetic abnormalities, including one with tetraploid karyotype and two with complex karyotype. But no consistent clonal abnormalities were described [4].

Recently, we and another group reported 2 small series of a total of 10 cases of ANKL that were EBV-negative. This type of NK-cell neoplasm preferentially occurs in non-Asians, and patients often present with systemic symptoms, hepatosplenomegaly, and progressive cytopenias. The clinical course is highly aggressive and often associated with hemophagocytic lymphohistiocytosis (HLH) [5,6]. The genetic alterations of the newly described EBV-negative ANKL are largely unknown. Nicolae et al. [5] reported missense mutations in the *STAT3* gene in 2 of 7 cases studied; however, this was not observed in our previously reported cases [6]. Three of the 12 cases of ANKL in the study by El Hussein et al. [4] were EBV negative, among which 2 had sequencing data and showed *TP53* and *ASXL2* mutations in one case with no JAK-STAT pathway mutations identified. In the present study, we performed comprehensive molecular genetic studies, including conventional cytogenetic analysis, fluorescence in situ hybridization (FISH), SNP microarray, and next-generation sequencing (NGS), on 4 cases of EBV-negative ANKL diagnosed in our institution. Our study reveals that our cases of EBV-negative ANKLs have complex genomic profiles including near-triploid/near-tetraploid karyotypes, inactivation of *TP53*, strong expression of c-Myc and PD-L1, and amplifications of *MYC* and *PDL1* genes.

2. Materials and methods

2.1. Cases

This study was approved by the Institutional Review Board of Northwestern University. Four cases that fulfilled the diagnostic criteria for ANKL based on the 2016 World Health Organization (WHO) classification but were EBV negative were included in this study [1].

2.2. Flow cytometric immunophenotyping

Flow cytometric analysis was performed on the bone marrow aspirate or lymph node tissue. Data collection was performed on a Becton Dickinson Biosciences (BD; Franklin Lakes, NJ) FACSCanto II flow cytometer. Data analysis was performed using FACSDiva software (BD). The following antibodies were used to assess T and NK cells: CD3 PerCP-Cy5.5 (clone SK7; BD), CD2 PC7 (clone 39C1.5; Beckman Coulter, Pasadena, CA, USA), CD5 APC (clone L17F12; BD), CD7 PE (clone 8H8.1; Immunotech, Ocala, FL, USA), CD4 FITC (clone SFCI12T4D11; Beckman Coulter), CD8 APC-H7 (clone SKI; BD), CD57 FITC (clone NCI; Beckman Coulter), CD56 PE-Cy7 (clone NKH-1; Beckman Coulter), CD16 PE (clone B73.1; BD), TIA1 PE (clone 2G9A10F5; Beckman Coulter), granzyme B FITC (clone GB11; BD), perforin FITC (clone δG9; BD Pharmingen, San Diego, CA, USA), TCR αβ (clone WT31; BD), TCR γδ (clone 11F2; BD), CD158a APC (clone EB6B; Beckman Coulter), CD158b FITC (clone CH-L; BD), and CD158e PE (clone Z27.3.7; Beckman Coulter).

2.3. Immunohistochemistry

Immunohistochemical staining was performed on the automated Ventana Benchmark (Ventana System, Tucson, AZ) or on automated Leica Bond Max (Leica Microsystems, Buffalo Grove, IL) using the Bond polymer refine detection horseradish peroxidase (HRP) (DS9800; Leica Biosystems, Lincolnshire, IL, USA) method as described in the study by Gao et al [6]. The following antibodies were used: CD45 (dilution 1:300, clone: 2B11+PD7/26; Dako, Glostrup, Denmark), predilute CD3 (clone LN10; Leica), CD20 (dilution 1:1000, clone L26; Dako), PAX5 (dilution 1:10, clone SP34; Cell Marque, Rocklin, CA, USA), predilute CD4 (clone 4B12; Leica), CD8 (dilution 1:40, clone C8/144B; Dako), CD2 (dilution 1:20, clone AB75; Leica), CD5 (dilution 1:40, clone 4C7; Leica), predilute CD7 (clone LP15; Leica), TCRγ (clone γ3.20; Thermo Fisher Scientific), TIA1 (dilution 1:150, clone 2G9A10F5; Beckman Coulter), predilute CD56 (clone CD564; Leica), βF1 (dilution 1:40, clone 8A3; Thermo Fisher Scientific, Mt Prospect, IL, USAr), CD30 (clone Ber-H2; Dako), EBER (predilute Eber 1 DNP Probe; Ventana), p53 (predilute, clone Bp53-11; Ventana), PD-L1 (dilution 1:50, clone SP142S; Spring BIoscience, Pleasanton, CA, USA), and c-Myc (pre-diluted clone EP121; Cell Marque).

2.4. Cytogenetic studies and FISH

Conventional cytogenetic analysis using the G-banding method was performed on fresh bone marrow aspirate samples after 24-hr or 48-hr unstimulated cultures following the standard protocol. At least 20 metaphase cells were examined in each case, and the chromosomal

abnormalities were described as per the International System for Human Cytogenetic Nomenclature (ISCN 2016).

Interphase FISH analyses assessing *MYC* and CD274 (*PDL1)*/PDCD1LG2 (*PDL2)* genes for rearrangement or copy number alterations (CNAs) were performed on formalin-fixed, paraffin-embedded tissue. A total of 100 interphase cells were evaluated, and negative and positive controls were evaluated in parallel with the patient samples in the same hybridization process. For *MYC* gene analysis, dual-color break-apart *MYC* probes (Abbott Molecular, Des Plaines, IL) consisting of the 5′ probe labeled with SpectrumOrange and the 3′ probe labeled with SpectrumGreen were used. Rearrangement of the *MYC* gene was determined by the percentage of cells with a separation of the 5′ and 3′ signals and compared with the cutoff value. Amplification of the *MYC* gene was defined in this study as $\geq$5 intact signals at the *MYC* locus. For CD274 (*PDL1)/PDCD1LG2(PDL2*) analysis, the probes targeting CD274 (labeled as spectrum orange, Empire Genomics, Buffalo, NY, USA), *PDCD1LG2* (labeled as spectrum green, Empire Genomics), and centromere 9 (CEP9, labeled as aqua, Abbott) were used. Cases were considered positive for *CD274*/*PDCD1LG2* amplifications when the *CD274*/*PDCD1LG2*-to-CEP9 ratio was $\geq$3.

2.5. SNP microarray analysis

Genomic DNA was extracted using a Qiagen DNeasy Blood and Tissue Kit (Qiagen, Valencia, CA), following the manufacturer's instructions. Chromosomal microarray analysis was performed using Affymetrix SNP microarray OncoScanTM HD arrays (Affymetrix/Thermo Fisher Scientific, Santa Clara, CA, USA) and following the manufacturer's instructions. The data were analyzed using Chromosome Analysis Suite software from Affymetrix and NEXUS copy number analysis (BioDiscovery, El Segundo, CA, USA). CNAs including copy number gains/amplifications or losses and copy-neutral loss of heterozygosity were manually reviewed.

2.6. Next-generation sequencing

NGS analysis was performed retrospectively on DNA extracted from air-dried bone marrow aspirate smears in case 1 and paraffin-embedded tissue from cases 3 and 4. No material was available for case 2. NGS was performed using the (University of Chicago Medicine, Chicago, IL, USA) OncoPlus Test, a 1212-gene hybrid capture panel that was sequenced on an Illumina HiSeq instrument (Illumina, San Diego, CA, USA). The data were analyzed using a custom-developed pipeline that detected point mutations, insertions/deletions, and copy number variations. The technical details of this assay have been described in the study by Kadri et al [7]. The bioinformatics pipeline produced a list of annotated variants that have a depth of read of at least $\times$50 (with a Phred quality score $>$30). This pipeline filters out all variants with frequency $>$1% reported in 1000 Genome, Exome Aggregation Consortium, and Exome Sequencing Project databases, any variants that were in the UTR or upstream/downstream of the gene, variants with a synonymous coding effect, and variants within intronic regions, unless they result in splice site mutations. The pipeline also was set to filter out variants that have a mutant allele frequency of less than 10%; however, if needed, variants with a mutant allele frequency of less than 10% can be curated manually, as was carried out in this project for the specimen from case 1, which had a tumor burden of $\sim$15%.

3. Results

3.1. Clinical features

The 4 patients diagnosed with EBV-negative ANKL in our institution included 3 men and 1 woman, and the ages at diagnosis were 48, 67, 70, and 88 years, respectively. The ethnicities included 2 Caucasians, 1 African American, and 1 Hispanic. The clinical and laboratory findings of the 4 patients are summarized in Table 1.

The detailed clinicopathological features of cases 1 to 3 were described in our previous report focusing on clinical and morphologic features of the disease [8]. In summary, all three patients presented generalized symptoms including fever, fatigue, night sweats, nausea, and weakness. Laboratory at presentation showed pancytopenia. Imaging revealed marked splenomegaly and mild lymphadenopathy. Two of the three patients had extensive infectious workup, which was negative. The diagnosis of EBV-negative NK-cell leukemia/lymphoma was made by bone marrow or tissue biopsy and was made on autopsy in one patient (patient 3). All three patients' clinical conditions deteriorated rapidly. Patient 1 and 3 died on day 3 and day 7 after initial presentation before any treatment could be initiated. Patient 2 developed HLH, was treated for HLH, subsequently received treatment for lymphoma, and died 3 months after initial presentation. Patient 4 was a 70-year-old Hispanic male who presented with intermittent fevers, cough, night sweats, and unintentional weight loss, initially thought to be an infectious or inflammatory process. Imaging showed marked splenomegaly and diffuse lymphadenopathy. Bone marrow and lymph node biopsies revealed an abnormal lymphoid infiltrate morphologically and immunophenotypically consistent with EBV-negative NK-cell leukemia/lymphoma. The patient's clinical course progressed rapidly, and he developed HLH and multiorgan failure, and he died 3 weeks after presentation. A full-dose chemotherapy could not be initiated owing to severe liver dysfunction.

In summary, all 4 patients with EBV-negative ANKL demonstrated similar clinical presentations, including systemic symptoms (3 of 4), splenomegaly (4 of 4),

Table 1 Summary of clinical and laboratory findings of EBV-negative aggressive NK-cell leukemia/lymphoma.

Cases	Age/sex/race	Presentation	Imaging	Laboratory findings			Site of involvement	Immunophenotype	Treatment and outcome
				CBC	LDH	EBV serology/EBER			
1	67/M/Caucasian	Fever, fatigue, night sweats	Marked splenomegaly with mass lesions, mild lymphadenopathy, multiple lung nodules	Pancytopenia	Elevated	Neg/Neg	Peripheral blood, bone marrow	Atypical NK cell phenotype [6]	- Sepsis, respiratory failure, progressive cytopenias - Died on day 3 after presentation; no chemotherapy received
2	48/M/African American	Fever, night sweats, myalgia, headache	Marked splenomegaly, hepatomegaly, mild lymphadenopathy, diffuse bone marrow signal abnormality	Pancytopenia	Elevated	Neg/Neg	Peripheral blood, bone marrow, liver	Atypical NK cell phenotype [6]	- Sepsis, progressive cytopenias, HLH, acute kidney injury, and respiratory failure - HLH treated with etoposide and dexamethasone - Lymphoma treated with EPOCH - Died 3 months after initial presentation
3	88/F/Caucasian	Abdominal pain, nausea, weakness	Marked hepatosplenomegaly, mild lymphadenopathy	Pancytopenia	NA	NA/Neg	Autopsy showing involvement of the bone marrow, spleen, liver, kidney, and adrenal gland, with minimal or no involvement of other organs	Atypical NK cell phenotype [6]	- Multisystem organ failure, coagulopathy, progressive cytopenias, metabolic acidosis, and acute kidney injury - Died on day 7 of presentation; no chemotherapy received
4	70/M/Hispanic	Fever, night sweats, weight loss	Marked splenomegaly	Pancytopenia	Elevated	IgG+,IgM-/Neg	Peripheral blood, bone marrow, lymph node	Atypical NK cell phenotype	- Multiorgan failure, progressive cytopenia, HLH - HLH treated with etoposide and dexamethasone - Died 3 weeks after presentation - Full-dose chemotherapy could not be initiated owing to severe liver dysfunction.

Abbreviations: HLH, hemophagocytic lymphohistiocytosis; NA, not available; Neg, negative; EPOCH, etoposide, prednisone, vincristine (Oncovin), cyclophosphamide, and doxorubicin hydrochloride (hydroxydaunorubicin hydrochloride); CBC, complete blood count; LDH, lactate dehydrogenase; EBV, Epstein-Barr virus; NK, natural killer.

progressive cytopenias (4 of 4), HLH (2 of 4), and a highly aggressive clinical course with a fatal outcome (4 of 4).

3.2. Morphologic and immunophenotypic features

The morphologic findings and ancillary studies of 4 patients with EBV-negative ANKL are summarized in Table 1. The detailed findings of cases 1 to 3 were described in a previous report [6].

The additional case (case 4) included in this study demonstrated virtually identical morphologic features to prior cases. The peripheral blood and bone marrow aspirate showed occasional atypical large lymphocytes, some with highly irregular nuclei and cytoplasmic granules. Occasional macrophages with hemophagocytosis were noted in the bone marrow aspirate smears (Fig. 1). Flow cytometric immunophenotyping performed on the peripheral blood revealed a NKcell population, a subset of which showed higher side scatter. The NK cells were surface CD3-, CD56+, CD2+, CD5-, partial CD7+, CD4-, CD8-, partial CD16+, CD57-, TIA1+, granzyme+, and perforin+. The subset of NK cells with higher side scatter

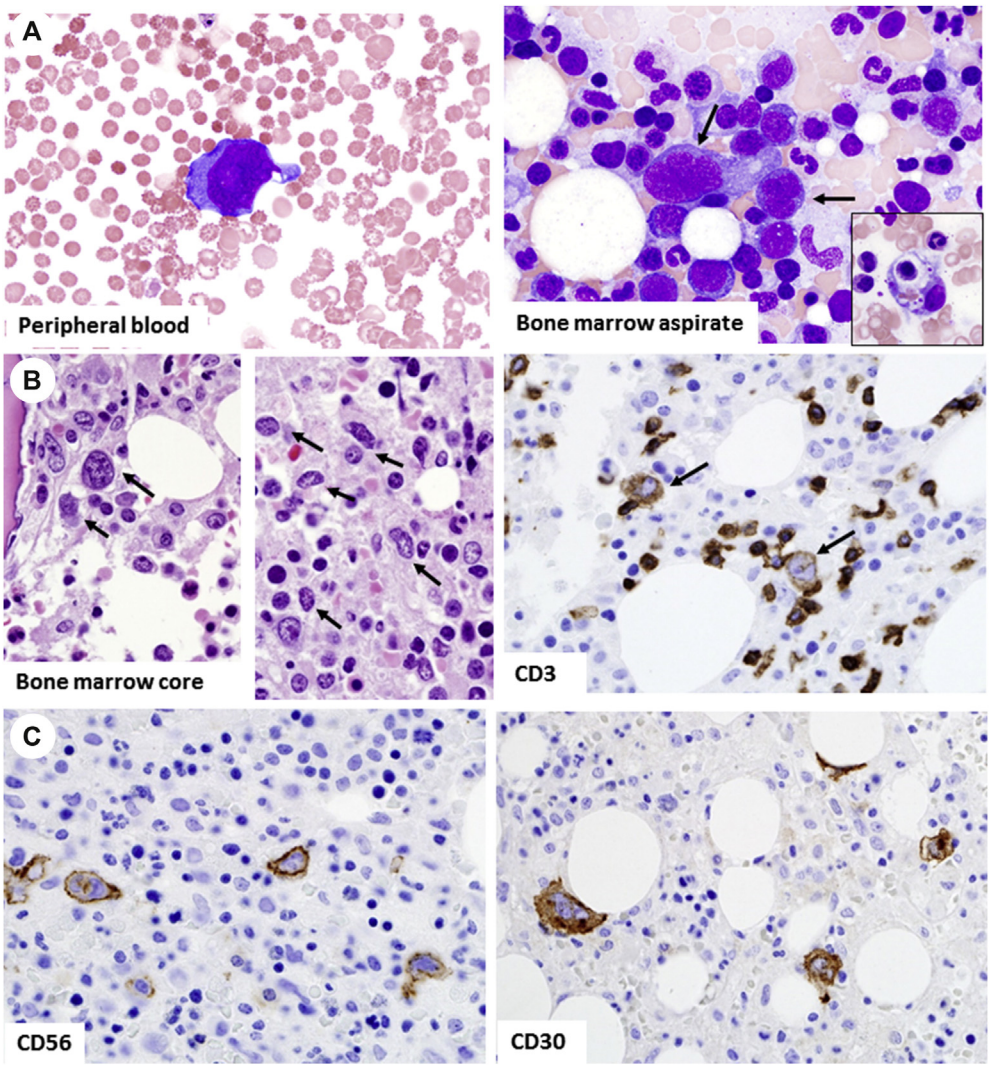

Fig. 1 Peripheral blood and bone marrow biopsy from patient 4. A, The peripheral blood smear shows rare large atypical lymphocytes with a large nucleus and prominent nucleolus (Giemsa, ×1000). The bone marrow aspirate smear shows multilineage hematopoiesis and occasional large atypical cells with large, irregular nuclei (Giemsa, ×1000). Rare hemophagocytosis is noted (inset; Giemsa, ×1000). B and C, The bone marrow core biopsy shows scattered atypical large cells with large nuclei and occasional prominent nucleoli (H&E, ×600). The atypical large cells are CD3+ (cytoplasmic staining), CD56+, and CD30+ (peroxidase, ×600). Additional immunostaining results show the neoplastic cells are CD2+, CD5-, CD7-, CD4-, and CD8- (not shown). Flow cytometric analysis performed on the peripheral blood revealed a NKcell population with atypical phenotype (see 3.2. Morphologic and immunophenotypic features). H&E, hematoxylin and eosin.

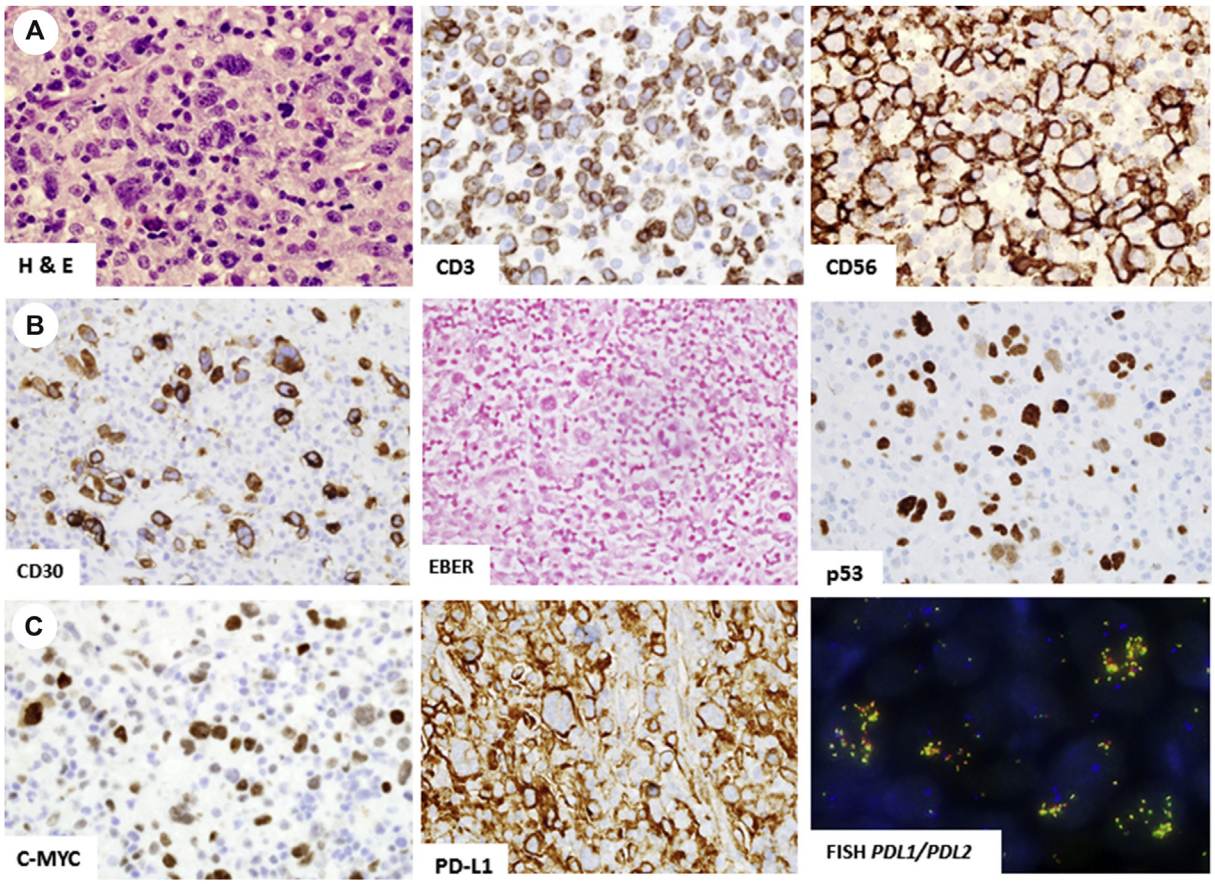

Fig. 2 Lymph node biopsy from patient 4. A, The H&E section (×400) shows effaced nodal architecture by diffuse infiltration of abnormal lymphocytes ranging from medium to large and highly pleomorphic cells. The neoplastic cells are CD3+ with a cytoplasmic staining pattern and strongly CD56+ (peroxidase, ×400). B, The neoplastic cells are CD30+ (peroxidase, ×400). In situ hybridization for EBER is negative (×400). P53 is positive in ∼60% of neoplastic cells. C, c-Myc is positive in ∼20% of cells. Programmed death-ligand 1 (PD-L1) is strongly positive in more than 90% of tumor cells. FISH shows *PDL1/PDL2* amplification (*PDL1*: green, *PDL2*: red, Cen 9: aqua). Additional immunostaining results show the neoplastic cells are CD2+, CD5-, CD7-, CD4-, CD8-, TIA1+, TCR BF1-, TCR delta-, CD20-, and PAX-5- (not shown). FISH, fluorescence in situ hybridization; H&E, hematoxylin and eosin.

showed atypical phenotype including negative staining for CD7 and heterogeneous loss of CD16 expression. Immunohistochemical staining on the bone marrow core biopsy revealed the atypical large cells were CD3+, CD2+, CD5-, CD7-, CD56+, CD4-, CD8-, and CD30+. In situ hybridization for EBER was negative. The findings were consistent with bone marrow involvement by EBV-negative ANKL. A subsequent cervical lymph node biopsy showed effaced nodal architecture by extensive lymphoid infiltrates composed of large, highly pleomorphic cells, some with multinucleation (Fig. 2). The large cells were positive for CD3, with a cytoplasmic staining pattern, CD2, CD56, CD30, and TIA1 and negative for CD5, CD7, CD4, CD8, CD20, PAX-5, TCR beta F1, and TCR delta. In situ hybridization for EBER was negative. In addition, approximately 60% of the neoplastic cells were positive for p53, 20% of the cells were positive for c-Myc, and more than 90% of the cells were strongly positive for PD-L1 (Fig. 2).

In summary, all 4 cases showed similar histologic and immunophenotypic features (Table 1) (Fig. 1) [6]. Overexpression of c-Myc and p53 was found in 4 of 4 cases and 3 of 4 cases (cases 1, 2, and 4), respectively. Strong expression of PD-L1 was observed in 60% of tumor cells in case 1 and in more than 90% of cells in case 4.

3.3. Genetic features

Conventional cytogenetic analysis was performed on the bone marrow aspirate specimens of two cases (cases 1 and 4) at the time of diagnosis. Both cases showed a highly complex, near-triploid/near-tetraploid karyotype with multiple numerical and structural abnormalities and marker chromosomes (Table 2 and Fig. 3). SNP microarray analysis performed on case 4 revealed segmental gains of 1q and 15q, gains of 6p/6q, and gains of Xp, Xq, and 11q (Fig. 4), as well as amplifications of chromosome 9p24.1 encompassing CD274 (*PDL1*), PDCD1LG2 (*PDL2*), and

Table 2 Genetic characteristics of EBV-negative aggressive NK-cell leukemia/lymphoma.

Cases	Cytogenetics	NGS results Mutated genes (VAF)	SNP Microarray	FISH for *MYC* and *PDL1/PDL2*	Immunohistochemistry
1	47−60,XY,+X,+Y,+1,ider(1)(q10)add(1)(q32),+3,+4,+6,+7,-9,+10,+11,+13,add(13)(q34),+14,+14,+18,+19,+20,add(21)(p11.3),+add(21)p11.1)x3,+mar1,+mar2+mar3[cp5]/83,idem,+X,+2,+3,+3,+5,+5,+6,+7,+8,+9,+9,+10,+11,del(11)(q23),+12,+add(13)(q34),+15,+16,+20,+22[3]/46,XY[12]	*DDX3X* p.I514T (12%) *LRRFIP*1 p.A645_A654del (5.5%) *TET2* p.P1894L (5.1%) *TET2* p.Q1903* (5.7%) *IDH2* p.R140Q (5.1%) *TP53* p.V197M (8.6%)	NA	NA (inadequate cells)	c-Myc: positive (50%) PD-L1: positive (60%) P53: positive (>90%)
2	NA	NA	NA	NA (inadequate cells)	c-Myc: positive (70%) PD-L1: positive in admixed histiocytes and rare tumor cells P53: positive (>90%)
3	NA	*FOXP1* p.Q173* (26%) *HIST1H3J* p.Q69* (16.5%) *SRSF3* p.F50Rfs*4 (25.6%) *TP53* p.L35* (20.9%)	All changes are related to triploid (3n) Copy number gains: 3, 4, 6p, 7q, 8q-ter (*MYC*), 10q26.13-ter, 11q23.2-ter (*MLL*, *CBL* and *CHEK1*), 13, 15 (with del15q), 18q22.3-ter, 19, 20p11.1-p11.23, 21, X Copy number losses: 4q35.1 (7.3 Mb) (*FAT1*), −5, 7p21.3-ter (11.6 Mb) (*CARD11*, *PMS2*, *RAC1*), 8p12-p11.2 (*NKX3*),11q22.3−23.2 (*ATM*, *SDHD*), 15q21.2, 17p13.1 (450 kb) (*TP53*, *GPS2*), 20q CN-LOH: Chr 5, 6p, 6q	*CD274/ PDCD1LG2:* consistent with triploid *MYC*: amplification	c-Myc: positive (40−50%) PD-L1: negative P53: negative
4	79−82,XY,i(X)(q10),-Y,-1,-2,add(2)(p13),add(3)(q25),-4,-4,add(4)(q31),add(5)(q31)x3,+6,add(6)(q13),i(6)(p10),-7,-8,add(8)(p11.2)x2,-9,-9,-10,-11,add(11)(q23)x2,-12,-13,-13,-13,add(13)(p11.2),-15,-16,-17-17,add(17)(p11.2),-18,-19,+21,add(22)(p11.1),add(22)(p11.2),+7−10mar[cp9]/46,XY[11]	*SETBP1* p.T228Sfs*8 (46%)	Copy number gains: 1q23.3 (5 Mb) (*SDHC*, *DDR2*, *DUF2*, *PBX1*), 6p, 6q23.3-ter, 9p24.2 (3 Mb) (*CD274, PDCD1LG2*, *JAK2*); 9p21.2 (3 Mb) (*LINGO2*, *TEK*), 11q23.3-ter (22 Mb) (*MLL*, *CBL* and *CHEK1*) 15q21.3 (2 Mb) (*TCF*12), 15q24.1 (5 Mb) (*MAP2K1*, *SMAD3* and *CD276*), 17p11.2 (*NCRO1*), Xpter (12 Mb)(*CRLF2*/*P2RY8*, *ZRSR2*), Xq Copy number losses: 17p13.2-ter (*TP53*), 22q11.23 (44 kb) (*SMACB1*) CN-LOH: Chr 4, 6q12-q22.33	*CD274/ PDCD1LG2*: amplification *MYC*: normal	c-Myc: positive (20%) PD-L1: positive (>90%) P53: positive (60%)

Abbreviations: CN-LOH, copy-neutral loss of heterozygosity; NGS, next-generation sequencing; NA, not available; VAF, variant allele frequency; FISH, fluorescent in situ hybridization; EBV, Epstein-Barr virus; NK, Natural killer; PD-L1, Programmed death-ligand 1.

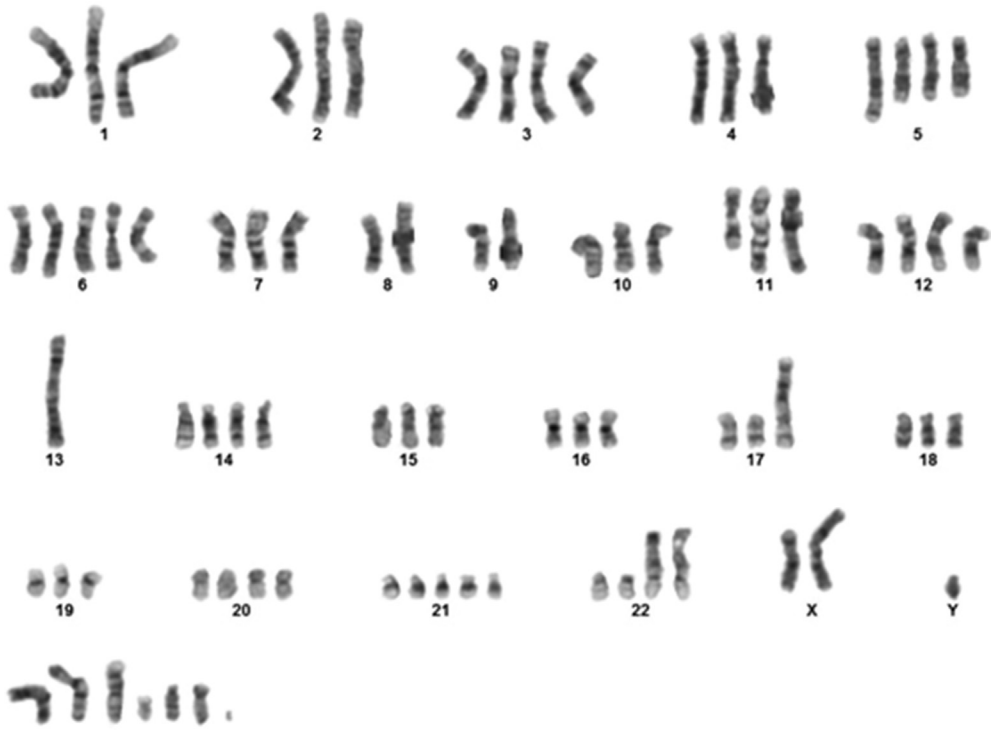

Fig. 3 Cytogenetic analysis performed on the bone marrow aspirate from patient 4 reveals a near-tetraploid karyotype with multiple numerical and structural chromosome abnormalities involving almost all chromosomes and several marker chromosomes of unknown origin.

JAK2. Given the karyotype of near-tetraploidy of the case, these findings of SNP microarray likely represent a near-tetraploid karyotype, which was automatically normalized to a diploid setting. Although chromosomal analysis was not performed on case 3 owing to lack of fresh tissue, SNP microarray analysis identified a near-triploid clone with multiple chromosome copy number alterations (CNAs) including gains of chromosomes 3, 4, 6p, 7q, 8q (encompassing the *MYC* locus), 11q, 13, 15, 19, 21, and X and losses of 4q, 5, 7p, 8p11q22.3−23.2, 15q, 17p13.1, and 20q (Table 2 and Fig. 4). Cases 3 and 4 shared a common gain of the 11q23-ter region and deletion of *TP53*.

FISH studies for *MYC* and *CD274 (PDL1)/PDCD1LG2 (PDL2)* were performed on 2 cases with available materials (cases 3 and 4). No *MYC* rearrangement was identified, but amplification of *MYC* was found in case 3. The corresponding immunostaining result showed c-Myc expression in 40−50% of tumor cells in case 3 and 20% of cells in case 4 (Fig. 2) [6]. Amplification of *CD274/PDCD1LG2* was detected in case 4 by FISH, consistent with the SNP microarray results and corresponding to the strong PD-L1 expression in the majority of neoplastic cells in this case (Fig. 2).

NGS was retrospectively performed on cases 1, 3, and 4. The results are summarized in Table 2. *TP53* mutations were identified in 2 cases (cases 1 and 3), including a *TP53* missense mutation in case 1 and nonsense mutation in case 3. In addition, mutations in *DDX3X*, *LRRFIP1*, *TET2*, and *IDH2* were identified in case 1. *TET2* p.Gln1903* and *IDH2* p.Arg140Gln are pathogenic mutations commonly seen in hematopoietic neoplasms, but coexistence of *IDH1/2* and *TET2* mutations is rare. Given that *TET2* is one of the most commonly observed mutations in normal individuals with advanced age [8], the possibility of *TET2* mutations representing clonal hematopoiesis of indeterminate potential cannot be completely excluded. In addition to *TP53*, case 3 harbored several pathogenic mutations including nonsense mutations involving *FOXP1* and *HIST1H3J* and frameshift mutation involving *SRSF3*. Case 4 had only a frameshift mutation in *SETBP1*.

4. Discussion

ANKL is a distinct entity in the WHO Classification of Tumors of Hematopoietic and Lymphoid Tissues, characterized by a neoplastic proliferation of mature NK cells that are usually EBV positive [1]. Patients often present with B symptoms, lymphadenopathy, hepatosplenomegaly, cytopenias with circulating leukemic cells, coagulopathy, hemophagocytic syndrome, and liver dysfunction. The clinical course is very aggressive, and patients often die within months. ANKL is highly associated with EBV infection and commonly occurs in East Asia.

Recently, two series of a total of 10 cases of EBV-negative ANKL were reported by us and another group, and

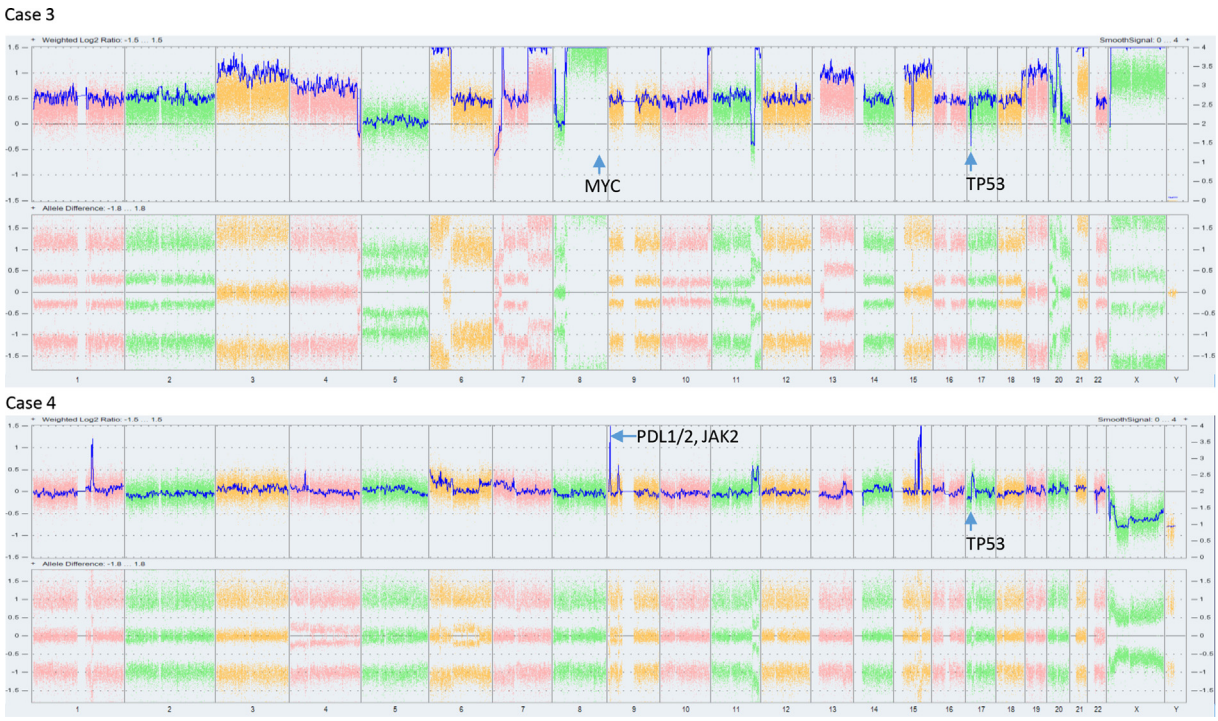

Fig. 4 Single nucleotide polymorphism (SNP) microarray whole-genome view of cases 3 and 4. A, Case 3 shows a triploid clone with multiple additional chromosomal gains and losses including gains of chromosomes 3, 4, 6p, 7q, 8q (encompassing *MYC* locus), 11q, 13, 15, 19, 21, and X. Deletion in 17p13.1 (*TP53*) is also identified (arrow). B, Case 4 shows a tetraploid genome that is normalized to a diploid setting with additional gains in 1q, 6p/6q, 11q, 15q, Xp, and Xq. In addition, amplification of 9p24.1 (*CD274*, *PDCD1LG2*, and *JAK2*) and deletion of 17p13.2-ter (*TP53*) are also identified (arrows). These 2 cases share common abnormalities of gain of the 11q23-ter region and deletion of the *TP53* gene.

both studies showed the EBV-negative ANKL preferentially affects non-Asians in contrast to EBV-positive ANKL. Patients often present with systemic symptoms, hepatosplenomegaly, and progressive cytopenias. The clinical course is highly aggressive and often associated with HLH [5,6]. EBV-negative ANKL is rare but could be under-recognized. The acute presentation of fever and splenomegaly often results in an extensive workup for infectious or inflammatory etiology. Morphologically, 3 of 4 cases in our series showed almost identical features. The neoplastic cells were highly pleomorphic and medium to large in size, some resembling megakaryocytes in the bone marrow biopsy. The neoplastic infiltrate in the bone marrow can be subtle and often masked by HLH. In addition, the atypical NK-cell phenotype, including very weak CD3 staining in some cases and EBER negativity, makes early diagnosis in the bone marrow difficult. However, CD56 staining is consistently positive and readily highlights subtle neoplastic infiltrates in the marrow. In addition, CD30 is often positive in the large neoplastic cells. The diagnosis of EBV-negative ANKL in our study was based on the morphologic evaluation, comprehensive flow cytometric analysis, and a battery of immunohistochemical staining markers [6]. The high index of suspicion enabled us to recognize an additional case (case 4) of EBV-negative ANKL in a bone marrow biopsy with a subtle infiltrate, and the diagnosis was further confirmed by a lymph node biopsy.

Previous studies have reported that molecular alterations in EBV-positive ANKL involve several key signaling pathways. Mutational analysis demonstrated frequent somatic mutations including *STAT3*, *STAT5*, *JAK2*, *JAK3*, *STAT6*, *SOCS1*, *SOCS3*, and *PTPN11,* resulting in an upregulated JAK/STAT-MYC axis [2]. Additional alterations were reported in the RAS-MAPK pathway and in epigenetic modifiers in EBV-positive ANKL [3]. Copy number gains spanning the *CD274 (PD-L1)/PDCD1LG2 (PD-L2)* loci and overexpression of p53 and c-Myc have also been reported [2,3]. Clonal cytogenetic abnormalities were also reported in 5 of 9 EBV-positive ANKLs, including one with tetraploid karyotype and 2 with complex karyotype [4].

Our present study focused mainly on the genetic alterations of EBV-negative ANKL as the current knowledge in this area is very limited. Nicolae et al. [5] reported missense mutations in the *STAT3* gene in 2 of 7 cases of EBV-negative ANKL, but this was not observed in our previous study [6]. In the present study, we performed comprehensive molecular genetic analyses, including conventional cytogenetic analysis, FISH, SNP microarray, and NGS, on 4 cases of EBV-negative ANKL diagnosed in our institution. We demonstrated highly complex karyotype in

3 of 3 cases characterized by near-triploidy/near-tetraploidy. Near-triploidy (58−80 chromosomes) and near-tetraploidy (81−103 chromosomes) are uncommon in hematopoietic neoplasms [9]. In a large study reported by Watanabe et al. [9], near-triploidy/near-tetraploidy was identified in 31 of 979 (3.2%) adult hematologic malignancies, including 11 of 398 (2.8%) B-cell neoplasms (6 diffuse large B-cell lymphomas, 2 plasma cell myelomas, 2 follicular lymphomas, and 1 B-cell lymphoma unclassifiable), 7 of 32 (21%) Hodgkin lymphomas, and 5 of 86 (5.8%) T-cell lymphomas (3 anaplastic T-cell lymphomas, 1 peripheral T-cell lymphoma unspecified, and 1 adult T-cell leukemia/lymphoma), among others (8 myeloid neoplasms). It is unclear whether NK/T-cell neoplasms were included in that study; nevertheless, the results demonstrated that near-triploidy/near-tetraploidy is uncommon in lymphomas. Our study revealed 3 of 3 cases of EBV-negative ANKL demonstrating the near-triploid/near-tetraploid karyotype. It is interesting that 3 of 4 cases in our series show almost identical morphology with frequent, highly pleomorphic giant tumor cells, some with multinucleation. This morphologic feature is not typically seen in EBV-positive ANKL and likely reflects the underlying cytogenetic abnormality of near-triploid/near-tetraploid karyotypes. It should be noted that the 3 EBV-negative ANKL cases in a recent series by El Hussein et al. [4] all had normal karyotypes. It is unclear whether the tumor burden plays a role in the discrepancy between our study and the study by El Hussein et al. [4].

Near-triploid/near-tetraploid karyotypes are complex, and the precise numerical and structural abnormalities can be difficult to be discerned by conventional karyotype analysis. In this study, SNP microarray was also performed on 2 cases (cases 3 and 4) to further identify subtle or cryptic genomic imbalances. One case (case 4) showed amplification of 9p24.1 spanning *CD274 (PD-L1)/PDCD1LG2 (PD-L2)* loci in addition to several other small interstitial chromosomal gains or losses, whereas the other (case 3) had frequent additional chromosomal or regional gains or losses, including gain of the *MYC* locus. In addition to *CD274* and *PDCD1LG2*, JAK2 is also one of the key genes located in chromosome 9p24.1, Genomic amplification at 9p24.1 may result increased expression of the key genes including *JAK2* and an upregulated JAK/STAT, which is often disturbed in EBV-positive ANKL. The SNP microarray results of these two cases shared some common abnormalities, including 17p deletion (encompassing the *TP53* locus) and gain of the 11q23-ter region. The gain of 11q23-ter has not been reported as a common copy number change in EBV-positive NK-cell neoplasms [10−12]. This region includes several important oncogenes such as *MLL*, *CBL*, and *CHEK1*. Gain of function of *MLL* and *CBL* is seen in myeloid neoplasms and less commonly seen in acute lymphoblastic leukemia [13,14]. *CHEK1* encodes a protein Chk1 in the serine/threonine protein kinase family. Activation of Chk1 induced by DNA damage can facilitate checkpoint-mediated cell cycle arrest and DNA repair. Overexpression of Chk1 has been shown in many solid tumors including breast, colon, liver, gastric, and nasopharyngeal carcinoma [15]. The specific roles of these oncogenes in lymphomagenesis remain to be elucidated.

TP53 is a well-known tumor suppressor gene that is mutated in various malignancies, including 47−63% of EBV-positive NK/T-cell lymphomas [16,17] and 34% of EBV-positive ANKLs [2]. *TP53* mutation in EBV-positive NK/T-cell lymphoma is often associated with the advanced stage and worse clinical outcome [18]. In the present study on EBV-negative ANKL, *TP53* alterations were seen in 4 of 4 cases, including *TP53* deletion and/or mutations, and overexpression of p53 was assessed by immunohistochemistry. In addition to *TP53* deletion, case 3 also harbored a *TP53* nonsense mutation in the other allele. This case illustrates a typical two-hit mechanism of loss of function of the *TP53* gene. Case 1 showed a *TP53* missense mutation (p.V197M), which has been reported in a variety of tumor types (COSMIC). These results suggest that loss of function or haploinsufficiency of *TP53* is an important oncogenic event in EBV-negative ANKL.

Similar to EBV-positive ANKL that is highly aggressive and refractory to chemotherapy, EBV-negative ANKL also shows a fulminant clinical course. Two of our 4 patients died within the first week of initial presentation, and one died 3 weeks and another died 3 months after initial presentations despite intensive chemotherapy. Alternative therapy is urgently needed for treatment of this aggressive neoplasm. In the present study, we found strong PD-L1 expression in the majority of neoplastic cells in 2 of 4 cases, and another case showed expression of PD-L1 in the admixed histiocytes. Two cases with available materials were subjected to FISH analysis, one of which showed amplification of *CD274 (PDL1)* and *PDCD1LG2 (PDL2)* loci. Programmed cell death protein 1 (PD-1)/Programmed death-ligand 1 (PD-L1) belongs to the family of immune checkpoint proteins that serve as coinhibitory factors to limit the T-cell−mediated adaptive immune response. Many cancer cells overexpress PD-L1, which deactivates the T-cell immune response in the tumor microenvironment. In recent years, cancer immunotherapy using checkpoint inhibitors has made remarkable progress. Blocking this inhibitory pathway may activate dormant T cells directed at cancer cells. Given the strong expression of PD-L1 observed in our EBV-negative ANKL, immune checkpoint therapy may be further explored as a potential therapeutic option for this aggressive NK-cell neoplasm.

In summary, we performed a comprehensive molecular genetic study on EBV-negative ANKL, a rare aggressive entity for which limited genetic data are available. Our cases of EBV-negative ANKL showed a highly complex, near-triploid/near-tetraploid karyotype, inactivation of *TP53*, overexpression of c-Myc, amplification of *CD274 (PDL1)*, and/or strong expression of PD-L1. All these features have been similarly reported in EBV-positive ANKL, which suggests that EBV-

positive and EBV-negative ANKL may share some common molecular mechanisms. Neither did we identify any *STAT3* mutations nor did El Hussein et al. [4] identify any *STAT3* mutations in their 2 of 3 EBV-negative ANKL cases with available sequencing data; however, this could be due to the relatively small number of cases studied. Amplification of 9p24.1 leads to increased expression of the key genes contained in this region, including *CD274 (PD-L1), PDCD1LG2 (PD-L2)*, and *JAK2*. The latter may result in upregulation of the JAK/STAT pathway, a key pathway that is altered in EBV-positive ANKL [2]. The strong expression of PD-L1 in the neoplastic cells suggests that immune checkpoint inhibitors may be further explored as a potential therapeutic option for this highly aggressive, chemotherapy-resistant NK-cell neoplasm.

References

[1] Chan JK, Jaffe ES, Ko YH. Aggressive NK-cell leukaemia. In: Swerdlow SHCE, Harris NL, et al., editors. WHO classification of tumours of haematopoietic and lymphoid tissues. Lyon: WHO Publications Center; 2017. p. 353–4.

[2] Huang L, Liu D, Wang N, et al. Integrated genomic analysis identifies deregulated JAK/STAT-MYC-biosynthesis axis in aggressive NK-cell leukemia. Cell Res 2018;28:172–86.

[3] Dufva O, Kankainen M, Kelkka T, et al. Aggressive natural killer-cell leukemia mutational landscape and drug profiling highlight JAK-STAT signaling as therapeutic target. Nat Commun 2018;9:1567.

[4] El Hussein S, Patel KP, Fang H, et al. Genomic and immunophenotypic landscape of aggressive NK-cell leukemia. Am J Surg Pathol 2020;44:1235–43.

[5] Nicolae A, Ganapathi KA, Pham TH, et al. EBV-negative aggressive NK-cell leukemia/lymphoma: clinical, pathologic, and genetic features. Am J Surg Pathol 2017;41:67–74.

[6] Gao J, Behdad A, Ji P, Wolniak KL, Frankfurt O, Chen YH. EBV-negative aggressive NK-cell leukemia/lymphoma: a clinical and pathological study from a single institution. Mod Pathol 2017;30:1100–15.

[7] Kadri S, Long BC, Mujacic I, et al. Clinical validation of a next-generation sequencing genomic oncology panel via cross-platform benchmarking against established amplicon sequencing assays. J Mol Diagn 2017;19:43–56.

[8] Busque L, Patel JP, Figueroa ME, et al. Recurrent somatic TET2 mutations in normal elderly individuals with clonal hematopoiesis. Nat Genet 2012;44:1179–81.

[9] Watanabe A, Inokuchi K, Yamaguchi H, et al. Near-triploidy and near-tetraploidy in hematological malignancies and mutation of the p53 gene. Clin Lab Haematol 2004;26:25–30.

[10] Iqbal J, Kucuk C, Deleeuw RJ, et al. Genomic analyses reveal global functional alterations that promote tumor growth and novel tumor suppressor genes in natural killer-cell malignancies. Leukemia 2009;23:1139–51.

[11] Ko YH, Choi KE, Han JH, Kim JM, Ree HJ. Comparative genomic hybridization study of nasal-type NK/T-cell lymphoma. Cytometry 2001;46:85–91.

[12] Nakashima Y, Tagawa H, Suzuki R, et al. Genome-wide array-based comparative genomic hybridization of natural killer cell lymphoma/leukemia: different genomic alteration patterns of aggressive NK-cell leukemia and extranodal Nk/T-cell lymphoma, nasal type. Genes Chromosomes Cancer 2005;44:247–55.

[13] Poppe B, Vandesompele J, Schoch C, et al. Expression analyses identify MLL as a prominent target of 11q23 amplification and support an etiologic role for MLL gain of function in myeloid malignancies. Blood 2004;103:229–35.

[14] Sanada M, Suzuki T, Shih LY, et al. Gain-of-function of mutated C-CBL tumour suppressor in myeloid neoplasms. Nature 2009;460:904–8.

[15] Zhang Y, Hunter T. Roles of Chk1 in cell biology and cancer therapy. Int J Canc 2014;134:1013–23.

[16] Zhang Y, Li C, Xue W, Zhang M, Li Z. Frequent mutations in natural killer/T cell lymphoma. Cell Physiol Biochem 2018;49:1–16.

[17] Li T, Hongyo T, Syaifudin M, et al. Mutations of the p53 gene in nasal NK/T-cell lymphoma. Lab Invest 2000;80:493–9.

[18] Quintanilla-Martinez L, Kremer M, Keller G, et al. p53 Mutations in nasal natural killer/T-cell lymphoma from Mexico: association with large cell morphology and advanced disease. Am J Pathol 2001;159:2095–105.